Characterization of Amorphous Hydrogenated Carbon Using Solid-State Nuclear Magnetic Resonance Spectroscopy

Karen C. Bustillo*

Department of Materials Science and Engineering, University of California, Berkeley, California 94720

Mark A. Petrich[1] and Jeffrey A. Reimer

Department of Chemical Engineering, University of California, Berkeley, California 94720

Received August 14, 1989

Amorphous hydrogenated carbon films deposited from a radio frequency (rf) plasma discharge were characterized with respect to their local bonding configurations and resulting electrooptical properties. Films deposited at substrate temperatures of 66–256 °C were examined with interferometry, ellipsometry, infrared spectroscopy, spectrophotometry, and electron spin resonance. The carbon bonding configurations and hydrogen content were subsequently measured with solid-state nuclear magnetic resonance (NMR). Observation of carbon-13 allowed for quantitative determination of the ratios of sp^2:sp^3 coordinated carbon and hydrogenated to non-hydrogenated carbon. It was found that with increasing deposition temperature, the energy gap decreased from 2.6 to 0.9 eV. The hydrogen content was constant between 16 and 23 at. % in these films. The sp^2 fraction varied between 48 and 61% of total carbon but showed no trend as a function of deposition temperature. It is concluded that changes in hydrogen content or changes in average sp^2 carbon content are not necessary to vary the electronic band structure of this amorphous semiconductor. The density of the material dramatically increased as a function of increasing deposition temperature, and it is suggested that the film density contributes to controlling the energy gap of these films.

Introduction

Amorphous hydrogenated carbon (a-C:H) is a technologically important material because of its versatile properties: extreme hardness, optical transparency in the visible and near infrared regions, chemical inertness, and ease of fabrication into uniform thin films. Several classes of applications have evolved for these amorphous materials: optical coatings,[2] protective coatings,[3] and semiconducting devices.[4] Like its predecessor amorphous hydrogenated silicon (a-Si:H), a-C:H is a semiconductor with an "energy gap", the value of which depends on the film deposition conditions. The ability to control the magnitude of the energy gap, refractive index, and mechanical properties relies on an understanding of the ways in which various processing conditions affect the microstructure. The hydrogen content and distribution, ratio of sp^2:sp^3 carbon coordination, and distribution of sp^2-coordinated carbon atoms all ostensibly contribute to the resulting film properties.[5]

The role of hydrogen in a-Si:H is complex. In part, it passivates dangling bonds that otherwise can cause defect states in the energy gap.[6] The addition of hydrogen to a-C:H is even more complex. Because carbon can form double bonds, adding hydrogen is not the only way to repair a dangling bond. Passivation of a dangling bond via a hydrogen atom retains the sp^3 hybridization of the carbon atom, and hence the energy gap and hardness remain similar to those of a diamond-like material. Passivation via formation of a carbon–carbon double bond adds to the sp^2 character of the film, making its properties more graphite-like.

In the a-C:H system, the electronic properties are affected by the presence of both sp^2- and sp^3-hybridized orbitals. It has been proposed that the weaker π-bonded states lie closest to the Fermi level and will form both conduction and valence band states.[7] Theoretical calculations predict that medium-range correlations between sp^2 carbon atoms are responsible for varying the bandgap.[7] Experimental evidence for this clustering theory has been obtained by using resonant Raman spectroscopy.[8] Recently it has been suggested that the extended carbon network provides the material with its mechanical properties and can be distinguished from such π-bonded clusters which may define the electrooptical properties.[9] In this case the energy gap would not necessarily change as a function of the average short-range microstructure such as hydrogen content or sp^2:sp^3 ratio.

Solid-state nuclear magnetic resonance (NMR) is a powerful probe of the local bonding configurations in amorphous semiconductors.[10] In a-C:H, the ^{13}C chemical shifts are distinct for the sp^2 and sp^3 bonding configurations because the electronic environments of the singly bonded carbon atoms and doubly bonded carbon atoms are different. NMR, therefore, allows one to measure the ratio of sp^2:sp^3 carbon bonding. The NMR spectrum is quantitative in that the intensity of the magnetization is proportional to the number of NMR-active spins. Comparing the area of the Fourier-transformed peak of the sample under study with that of a standard having a known amount of spins allows one to calculate the number

(1) Current address: Department of Chemical Engineering, Northwestern University, Evanston, IL 60208.
(2) Bubenzer, A.; Dischler, B.; Brandt, G.; Koidl, P. *Opt. Eng.* **1984**, *23*, 153.
(3) Tsai, H.; Bogy, D. B. *J. Vac. Sci. Technol. A* **1987**, *5*, 3287.
(4) Noda, K.; Nakatsugawa, M.; Ninomiya, Y.; Itoh, T. *J. Appl. Phys.* **1987**, *62*, 3799.
(5) Robertson, J. *Adv. Phys.* **1986**, *35*, 317.
(6) Chittick, R. C.; Alexander, J. H.; Sterling, H. F. *J. Electrochem. Soc.* **1969**, *116*, 77.
(7) Robertson, J.; O'Reilly, E. P. *Phys. Rev. B* **1987**, *35*, 2946.
(8) Ramsteiner, M.; Wagner, J. *Appl. Phys. Lett.* **1987**, *51*, 1355.
(9) Tamor, M. A.; Wu, C. H.; Carter, III, R. O.; Lindsay, N. E. *Appl. Phys. Lett.* **1989**, *55*, 1388.
(10) Grill, A.; Meyerson, B. S.; Patel, V. V.; Reimer, J. A.; Petrich, M. *J. Appl. Phys.* **1987**, *61*, 2874.

0897-4756/90/2802-0202$02.50/0

of NMR-active nuclei in each chemical environment. The hydrogen content of the film can thus be measured with proton NMR.

In this work, the energy gap, or optical bandgap, was related to the carbon bonding configurations and the hydrogen content. The varying optical gaps were obtained by altering the deposition temperature of the samples. The carbon microstructure and hydrogen content were quantitatively investigated with solid-state nuclear magnetic resonance.

Experimental Section

Sample Preparation. Samples of a-C:H thin films were deposited in an rf plasma-assisted chemical vapor deposition (PACVD) reactor.[11] Two planar electrodes, 9 cm in diameter and separated by 3 cm, were capacitively coupled to a 13.6-MHz rf generator. Radio frequency power of 55 W (0.9 W/cm^2) was introduced via the bottom electrode, and the sample was pinned upside down to the top grounded electrode. Heating of this electrode was achieved with a variable resistive heater, and the temperature was controlled in the range 27–325 °C (±3 °C). The source gas was a mixture of 20 sccm CH_4 and 30 sccm H_2. Prior to deposition the system was evacuated to 10^{-5} Torr, and during deposition a butterfly value controlled the reactor pressure to 200 mTorr. The above process conditions were chosen after performing a matrix of experiments designed to maximize the deposition rate while achieving uniform films with good adhesion to the substrate. Silicon substrates were used for film thickness, refractive index, and infrared (IR) measurements. Quartz substrates were used for optical bandgap and film thickness measurements. Aluminum foil covered the sample electrode in all depositions and provided a convenient removable substrate for NMR and electron spin resonance (ESR) samples.

Film thickness was measured by using a combination of methods: ellipsometry for films 400–800 Å thick on silicon substrates, interferometry for films 0.1–1.0 μm thick on silicon substrates, and profilometry for films greater than 1.0 μm thick on quartz and silicon substrates. The real part of the refractive index was measured with an ellipsometer at a wavelength of 632.8 nm. IR spectra were taken at each sample temperature to ensure that oxygen had not been incorporated into the film during deposition. ESR was used to determine the average paramagnetic spin density in these samples.

Optical Bandgap Measurements. The optical bandgap was measured by using optical absorption and Tauc's approximation.[12] It is represented by $E_{g(opt)}$ in this paper. Six films with thickness between 1.6 and 2.7 μm were deposited on quartz substrates; two were deposited at 66 and 208 °C, and one each was deposited at 166 and 256 °C. A UV/vis/NIR spectrophotometer was used in the absorption mode to scan the samples in the wavelength range 320–720 nm. The quartz substrate was found to have a flat response over the entire scan range, and the absorption was small enough to be neglected. Effects due to thickness interference between the film interface and substrate were also ignored. Values of the absorption coefficient greater than 10^4 cm^{-1} were plotted as a function of photon energy, and straight lines were fit with a least-squares analysis. The energy gap was calculated at the value of zero absorption.

NMR Spectra. There are two dominant spin–spin relaxation mechanisms in the a-C:H system that determine the NMR experiments required and the line shapes observed: chemical shift interactions and direct dipole–dipole interactions. Both chemical shift and dipolar interactions contain an angular dependence with respect to the static magnetic field. Chemical shift anisotropy can be reduced by magic-angle spinning (MAS),[13,14] allowing distinction between chemically different sites. Even under MAS conditions, the presence of hydrogen in the amorphous hydrogenated carbon films dominates the transverse relaxation of carbon nuclei that are either directly bound or sufficiently close to a hydrogen atom. Sufficient proximity is determined by the r^{-3} dependence in the dipolar interaction.[15] All carbon atoms experiencing carbon–proton coupling will be described in this paper as hydrogenated.

Due to the strong heteronuclear dipolar interaction, the line shape from the hydrogenated carbon atoms is indistinguishable from the base line in a single-resonance spectrum. To distinguish the hydrogenated peaks, one can use double-resonance techniques to decouple the carbon–proton interaction. One method of decoupling is to irradiate the hydrogen nuclei with an rf field at their Larmor frequency during acquisition of the carbon free induction decay. Double-resonance decoupling experiments produce a spectrum that shows peaks arising from all carbon atoms, both hydrogenated and non-hydrogenated. Single-resonance experiments produce a spectrum with only non-hydrogenated carbon peaks visible.

Another double-resonance technique often referenced in the literature is cross polarization (CP).[16–19] Cross polarization uses the high gyromagnetic value of protons to enhance the magnetization of nearby carbon nuclei. It is important to note that cross polarization works only for hydrogenated carbon. Non-hydrogenated carbon atoms that appear in the single-resonance spectra in this study are most likely not observed in cross-polarization experiments. Remarks in the literature stating that it is not possible to measure isolated carbon with NMR are incorrect,[5,16,20] leading to misconceptions that NMR is not capable of establishing a ratio of sp^2:sp^3 carbon in non-hydrogenated material. Although time consuming, because the sensitivity is greatly reduced from what one observes with cross polarization, it is certainly possible to measure the ^{13}C signal in non-hydrogenated material with sufficient sample quantity and a large number of signal averages.

The probe used in all ^{13}C experiments was a broad-band double-resonance magic-angle spinning probe (Doty Inc.) with a 7-mm coil. The spectrometer used for the ^{13}C experiments was a home-built instrument operating at a carbon frequency of 45 MHz and a proton frequency of 180 MHz. The $\pi/2$ pulse length was 6 μs, the delay between acquisitions was 20 s, and the data were gathered from 2000 signal averages. The two spectral features corresponding to the sp^2 and sp^3 carbon and appropriate magic-angle-spinning sidebands were fit with Gaussian line shapes. Integration of the area under the sp^2 and sp^3 regions in the decoupled spectra yielded the sp^2:sp^3 ratio. Integration of the single resonance and decoupled spectra yielded the hydrogenated and non-hydrogenated fractions.

Proton spectra were obtained on a home-built NMR spectrometer operating at 267 MHz and on a commercial spectrometer (Nalorac Cryogenics Corp.) at 399 MHz. At 267 MHz the $\pi/2$ pulse length was 6 μs with a repetition delay of 20 s, and 100 signal averages were co-added. At 399 MHz, the $\pi/2$ pulse length was 2.7 μs with a repetition delay of 2 s, and 400 signal averages were co-added. Hexamethylbenzene and adamantane served as reference samples.

Both ^1H and ^{13}C NMR studies involved samples prepared at four different substrate temperatures: 66, 166, 208, and 256 °C. Optical bandgaps of 2.6, 2.1, 1.4, and 0.9 eV can be ascribed respectively to the four samples. Large amounts of material were required (5–100 mg), for both ^1H and ^{13}C experiments, to provide sufficient signal intensity. The films were deposited on aluminum foil and dissolved in a dilute HCl bath, leaving the a-C:H film fragments. One might argue that the process of dissolving the film from the substrate altered the bulk properties of the carbon film. However, the ratio of surface to bulk atoms was less than 2% for the size particles that were obtained, and so one can assume that most of the signal was due to bulk carbon. In ad-

(11) Knights, J. C. *Jpn. J. Appl. Phys.* **1979**, *18* (Supplement 18-1), 101.
(12) Tauc, J. *Amorphous and Liquid Semiconductors*; Plenum: New York, 1974.
(13) Andrew, E. R.; Bradbury, A.; Eades, R. G. *Nature (London)* **1958**, *182*, 1659.
(14) Lowe, I. J. *Phys. Rev. Lett.* **1959**, *2*, 285.
(15) Gerstein, B. C.; Dybowski, C. R. *Transient Techniques in NMR of Solids*; Academic Press: Orlando, FL, 1985.
(16) Kaplan, S., Jansen, F.; Machonkin, M. *Appl. Phys. Lett.* **1985**, *47*, 750.
(17) Kaplan, S.; Dilks, A. *Thin Solid Films* **1981**, *84*, 419.
(18) Jarman, R. H.; Ray, G. J.; Standley, R. W.; Zajac, G. W. *Appl. Phys. Lett.* **1986**, *49*, 1065.
(19) Yamamoto, K.; Echikawa, Y.; Nakayama, T.; Tawada, Y. *Jpn. J. Appl. Phys.* **1988**, *27*, 1415.
(20) Angus, J. C.; Hayman, C. C. *Science* **1988**, *241*, 913.

Table I. Quantitative Results from NMR Experiments

deposition temp, C°	$E_{g(opt)}$,[a] eV	hydrogen content at 267 MHz,[b] at. %	hydrogen content at 399 MHz,[b] at. %	fraction sp^2 carbon,[c] at. %	fraction non-hydrogenated carbon,[c] at. %	fraction diamond-like carbon,[c] at. %
66	2.6	23	22	55	51	13
166	2.1	22	18	57	35	11
208	1.4	21	16	48	58	28
256	0.9	21	21	61	65	16

[a] ±0.2 eV. [b] ±3 at. %. [c] ±8 at. %.

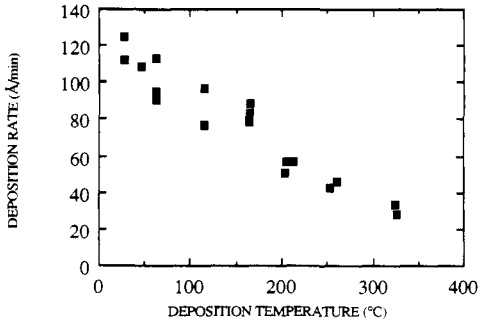

Figure 1. Deposition rate (Å/min) on silicon substrates as a function of deposition temperature. Deposition conditions: gas flow rates of 20 sccm CH_4 and 30 sccm H_2, reactor pressure of 200 mTorr, and rf power of 55 W.

dition, it is known that a-C:H is unreactive and impervious to a number of strong acids, including HCl.[2]

Results and Discussion

Film Characterization. The deposition rate, as measured by thickness per unit time, decreased dramatically as a function of deposition temperature of the substrate (Figure 1). Such behavior has been observed in fluorinated silicon nitride films.[21] The mass of the film deposited, as measured with an analytical balance, did not significantly change, however, for depositions at different substrate temperatures and deposition times of 8 h. These observations indicate that as the temperature increased, the volumetric density increased. Densification was obvious by qualitatively comparing the volumes of NMR samples with their associated masses. However, it is unlikely that changes in film density alone can account for the dramatic decrease in thickness at constant mass. It is expected that material sputtering competed with material deposition and that material was lost during the extended 8-h depositions. The sputtering rate may be a function of deposition temperature. At a given temperature, the deposition rate was constant for deposition times of 5 min to 2 h. It is not known whether the deposition rate was constant over periods of time longer than 2 h. Nevertheless, it is assumed that increased substrate temperature significantly densified the a-C:H films. Others have observed a decreasing film thickness with constant mass deposition in methane plasmas as a function of total power supplied by ions to the film. It was determined that the methyl radical flux largely determined the mass deposition rate while the power supplied to the surface via ion bombardment acted to densify the film.[22]

The real part of the refractive index, as measured on films 400–800 Å thick, was also seen to increase sharply from 1.7 to 2.0 coincident with an increase in substrate temperature from 27 to 100 °C. Above 100 °C the refractive index fluctuated between 2.0 and 2.3. An increase in the film refractive index often correlates with increased film density.[23]

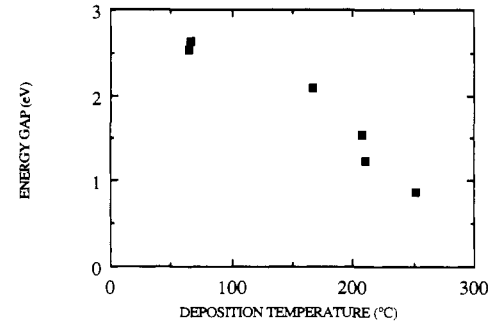

Figure 2. Energy gap (electronvolts) measured by optical absorption, as a function of deposition temperature.

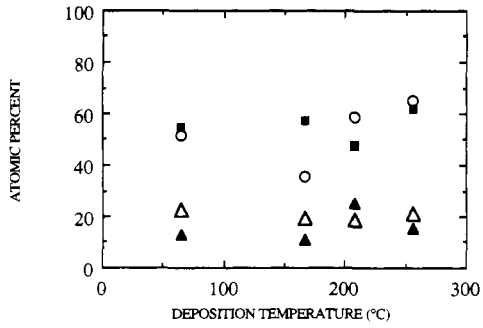

Figure 3. Results from NMR studies of a-C:H showing that the average carbon bonding configuration and the hydrogen content do not show trends as a function of deposition temperature. Graph shows non-hydrogenated carbon fraction (circles), diamond-like carbon (filled triangles), hydrogen content (open triangles), and sp^2-coordinate carbon fraction (squares).

The optical bandgap is plotted as a function of deposition temperature in Figure 2. As is evident, it decreased with increasing temperature as reported by others.[24,25] Because both film density and optical gap depend on substrate temperature, the two film properties may be related. Recently the density measurements from several investigations have been plotted as a function of optical gap and were found to correlate in the range 0.7–2.0 eV.[9]

The density of paramagnetic spins, as measured with ESR, was (6.0–6.6) × 10^{18} cm^{-3} in the 66, 166, and 208 °C samples and increased slightly to 8.4 × 10^{18} cm^{-3} in the 256 °C sample. The ESR spectra were observed near a g value of 2.0023, and the peak-to-peak line widths were measured to be 8–10 G. The localized unpaired electrons were presumed to be dangling bonds. ^{13}C nuclei adjacent to dangling bonds will couple to these unpaired electrons and will not be visible in the NMR spectrum. The measured

(21) Livengood, R. E.; Petrich, M. A.; Hess, D. W.; Reimer, J. A. *J. Appl. Phys.* **1988**, *63*, 2651.
(22) Vandentop, G. J.; Kawaski, M.; Nix, R. M.; Brown, I. G.; Salmeron, M.; Somorjai, G. A. *Phys. Rev. B*, in press.
(23) Dischler, B. *Amorphous Hydrogenated Carbon Films (Proc. E-MRS 1987)*; Les Éditions de Physique: Cedex, France, 1987.
(24) Anderson, D. A. *Philos. Mag.* **1977**, *35*, 17.
(25) Meyerson, B.; Smith, F. W. *J. Non-Cryst. Solids* **1980**, *35/36*, 435.

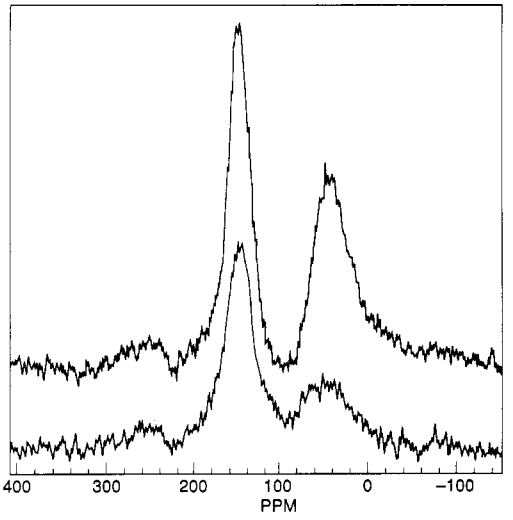

Figure 4. Example of decoupled (top) and single-resonance (bottom) ^{13}C NMR spectra. Film was deposited as 208 °C. MAS spinning was used with a rotor frequency of 4.5 kHz. The large peak at 145 ppm corresponds to sp^2-coordinated carbon, and the large peak at 40 ppm corresponds to sp^3-coordinated carbon. The small peak on the left is one of the spinning sidebands belonging to the sp^2 peak. The chemical shift axis is referenced to TMS.

paramagnetic spin density corresponded to less than 1% of the ^{13}C nuclei, and therefore the reduction in signal intensity was negligible.

Carbon Coordination. The ratios of sp^2:sp^3 carbon and of hydrogenated:non-hydrogenated carbon are displayed in Table I and Figure 3. It is evident that within experimental error, the sp^2:sp^3 ratio is approximately the same in all four samples. The sp^2-coordinated fraction varies from 48 to 61%, and the fraction of non-hydrogenated carbon varies from 35 to 65%. Neither ratio shows a monotonic dependence on deposition temperature and hence optical bandgap. It appears that hydrogen is most likely to bond to or be adjacent to an sp^3-coordinated carbon. This finding is contradictory to the previously published assumption that there is no preferential hydrogen bonding to a particular carbon coordination.[23] IR absorption studies have indicated that almost all hydrogenated carbon is sp^3-coordinated while most non-hydrogenated carbon is sp^2-coordinated.[9] It must be remembered that in this present study, non-hydrogenated is used to refer to a carbon nucleus that was sufficiently removed from a hydrogen nucleus to ignore the r^{-3} heteronuclear dipolar interaction. The fraction of diamond-like material, or sp^3 non-hydrogenated carbon, ranged from 11 to 28%. Measurement errors can largely be attributed to data smoothing and curve fitting in preparation for integration.

The sp^2- and sp^3-coordinated carbon chemical shifts with respect to tetramethylsilane (TMS) are located at approximately 145 and 40 ppm, respectively (Figure 4). The chemical shift for sp^1-hybridized carbon in acetylenic form should be located around 75 ppm with respect to TMS.[26] Such a peak would lie within the sp^3-hybridized carbon line shape, and consequently this study was not able to verify the existence of triply bonded carbon. It was reported from IR studies that the presence of sp^1 sites was less than 2% for an annealing temperature of less than 200 °C. This annealing temperature was associated with a deposition temperature of 100 °C. Below annealing temperatures of 200 °C, no evidence for triple-bond formation was found.[23] Other studies do not report the presence of triply bonded carbon atoms in films deposited from methane, and this study assumes the contribution to be small.

NMR was previously applied to one a-C:H sample by using techniques similar to those used in this study: MAS single resonance and MAS with proton decoupling.[10] The sample described in the report was deposited at 250 °C, and the sp^2 fraction was measured to be 62%. The non-decoupled spectrum indicated that no non-hydrogenated sp^3 carbon, and hence no "diamond-like" character, was present in the film.

Hydrogen Content. The observed proton NMR spectra show both a broad Gaussian component (150–160 ppm full width at half-height) and a narrow Lorentzian component (approximately 5–10% of the total spectra area). The Gaussian component is assigned to clusters of protons possessing strong ^1H–^1H coupling. The Lorentzian component is assigned to isolated hydrogen atoms (although the presence of H_2 in the gas phase cannot be precluded). Similar results have been obtained from proton NMR studies of a-Si:H[27] and of a-C:H.[28] The average hydrogen content for the deposition temperature range 66–256 °C is 20%. This is a low value of hydrogen content compared to many reports in the literature,[16,29] although others have reported even lower hydrogen contents.[30] It is clear that hydrogen content alone is not responsible for varying the bandgap of these samples. With such a wide range of bandgaps, one would expect hydrogen contents to vary be more than the observed 7 at. % to account for the 200% change in energy gap.

Conclusion

A survey of the literature revealed that explanation for the dependence of the optical bandgap in a-C:H films on plasma deposition parameters was not complete. It was expected that the value of the bandgap would be affected by either hydrogen content or fraction of π-bonded carbon atoms. This study reports that while the film appears to be more dense at higher deposition temperatures, the average bonding configuration does not change. The average number of single and double carbon bonds, the fractions of hydrogenated carbon for these two coordinations, and the hydrogen content remain constant. Yet the electrical properties, specifically the optical bandgap, have been greatly affected by the changes in the deposition temperature. The dramatic decrease in bandgap observed in this work correlates strongly with the sharp increase in volumetric density of the a-C:H films. It is suggested that in addition to carbon bonding configurations and hydrogen content, the film density contributes to control of the electrooptical properties of a-C:H materials.

Acknowledgment. We thank Paul Skerker for assistance with electron spin resonance measurements. K.C.B. acknowledges Professor Eugene Haller for his support. This work was supported by National Science Foundation Grants DMR-83-04163 and DMR-84-51234, Xerox Corp., and the Alcoa Foundation.

Registry No. C, 7440-44-0; H_2, 1333-74-0.

(26) Duncan, T. M. *J. Phys. Chem. Ref. Data* **1987**, *16*, 125.

(27) Gleason, K. K.; Petrich, M. A.; Reimer, J. A. *Phys. Rev. B* **1987**, *36*, 3259.

(28) Reimer, J. A.; Vaughan, R. W.; Knights, J. C.; Lujan, R. A. *J. Vac. Sci. Technol.* **1981**, *19*, 53.

(29) Fink, J.; Müller-Heinzerling, Th.; Pflüger, J.; Scheerer, B.; Dischler, B.; Koidl, P.; Bubenzer, A.; Sah, R. E. *Phys. Rev. B* **1984**, *30*, 4713.

(30) Couderc, P.; Catherine, Y. *Thin Solid Films* **1987**, *146*, 93.